Available online at www.sciencedirect.com
SCIENCE DIRECT
Tetrahedron 62 (2006) 8770–8778
Tetrahedron

A homologous series of eunicellin-based diterpenes from *Acalycigorgia* sp. characterised by tandem mass spectrometry

Kwaku Kyeremeh,[a] Thomas C. Baddeley,[a] Bridget K. Stein[b] and Marcel Jaspars[a,*]

[a]*Marine Natural Products Laboratory, Department of Chemistry, University of Aberdeen, Old Aberdeen, AB24 3UE, Scotland, UK*
[b]*EPSRC Mass Spectrometry Service Centre, University of Wales Swansea, SA2 8PP, Wales, UK*

Received 21 April 2006; revised 9 June 2006; accepted 29 June 2006
Available online 24 July 2006

Abstract—The discovery and structure determination of a homologous series of eunicellin-based diterpenes from the gorgonian *Acalycigorgia* sp. is described. Extensive use was made of 1D and 2D NMR data to determine the structure of the diterpene skeleton. The relative stereochemistry was confirmed via the use of NOE data in conjunction with molecular modelling. A series of homologues were identified using a combination of product and precursor ion scanning modes in tandem mass spectrometry. This powerful technique afforded excellent clarification to aid the analysis of the complex mass spectral data.

1. Introduction

Species of the class Alcyonaria produce a wealth of bioactive diterpenes, amongst which are the promising anti-cancer leads, the sarcodictyins and eleutherobin. The Mediterranean gorgonian *Eunicella singularis* (=*Eunicella stricta*) was the source of the unique marine diterpenoid eunicellin first reported by Djerassi's group in 1968.[1] Since then, many other species from the genera *Eunicella*,[2] *Cladiella*,[3] *Briareum*,[4] *Sarcodictyon*,[5] *Eleutherobia*,[6] *Solenopodium*,[7] *Sclerophytum*[8] and *Alcyonium*[9] have resulted in a very large number of marine diterpenoids based on the eunicellin skeleton. It appears that eunicellin-based diterpenoids are a very pronounced feature of the class Alcyonaria since the species that produce them have been collected from many locations around the world (Mediterranean, Atlantic, Indian and Pacific Oceans). Even though their exact ecological significance is still not certain, several ecological and agrochemical related activities have been reported for these diterpenes, including molluscidal and mollusc repellant activity,[10,11] hemolytic activity,[12] inhibition of cell division in fertilised starfish eggs[13] and insect growth inhibitory activity.[14] The structure, source and biological activities of the many known members of the cladiellins, briarellins, asbestinins and sarcodictyins have been reviewed by Paquette et al.[14] Pharmacologically, there is a significant relationship between the structure and activity of these diterpenoids; both sarcodictyins A and B and eleutherobin (the 'eleutheside' family of microtubule-stabilising compounds) are characterised by an activity profile different from that of the anti-cancer agent paclitaxel (Taxol™).[15] In particular, they are active against paclitaxel resistant tumour cell-lines. Theoretical pharmacophore studies on the various features of microtubule stabilising compounds taxol, epothilones, eleutherobin/sarcodictyin and laulimalides have led to the proposal of the hypothesis that the core ring systems and side chains present in these compounds might bind to common binding sites in β-tubulin, resulting in a similarity in their biological functions.[16,17] The apparent lack of activity amongst several eunicellin-based diterpenoids might only be due to the absence of appropriate side chain functional groups, which bind efficiently to sites in β-tubulin.

In this study we present the structures of a new homologous series of eunicellin-based diterpenoids from *Acalycigorgia* sp. The structures of these compounds were elucidated using 1D and 2D NMR and MS techniques. We extended the analysis of the homologous series by tandem mass spectrometry using precursor ion scans.

* Corresponding author. Tel.: +44 1224 272895; fax: +44 1224 272921; e-mail: m.jaspars@abdn.ac.uk

0040–4020/$ - see front matter © 2006 Elsevier Ltd. All rights reserved.
doi:10.1016/j.tet.2006.06.102

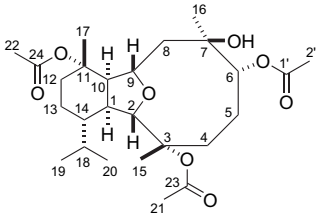

1

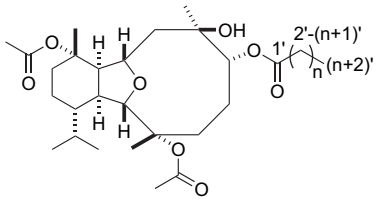

2a-t
n = 4-20

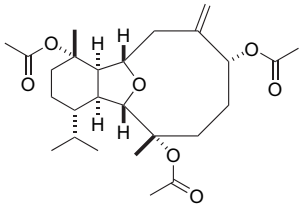

3

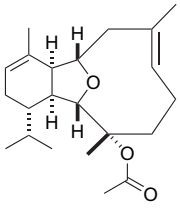

4

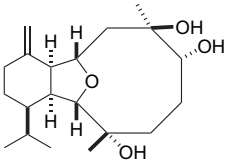

5

2. Results and discussion

The US National Cancer Institute's Open Repository Program provides our laboratory with crude extracts of marine invertebrates, which are screened for differential cytotoxicity at the Ford Cancer Center, Detroit, USA. As a part of this collaboration we had the opportunity to study the gorgonian *Acalycigorgia* sp. The sample of *Acalycigorgia* sp. was collected by the Australian Institute of Marine Science scientists in Thailand in June 1990 at 15 m. Solvent partitioning, followed by size exclusion, low- and high-pressure liquid column chromatographic procedures afforded two new eunicellin-based diterpenoids and an intractable mixture of homologues.

The ^{1}H NMR spectrum of compound **1** was characterised by eight methyl signals made up of three acetyl methyls at δ_H 2.04 (s, 3H), 1.99 (s, 3H), 1.95 (s, 3H), three vinyl methyls or methyls attached to oxygenated quaternary carbons at δ_H 1.45 (s, 3H), 1.33 (s, 3H), 1.20 (s, 3H) and an isopropyl group with two methyls at δ_H 0.94 (d, 3H, J=6.8 Hz) and 0.80 (d, 3H, J=6.8 Hz). The ^{13}C NMR of compound **1** was made up of 26 ^{13}C resonances in total. These data suggested that **1** was a marine diterpene with three acetate groups attached to the C_{20} skeleton. A database search on MarinLit[18,19] using the genus and information from 1D NMR indicated the likelihood of an eunicellin skeleton being present. Six quaternary carbon atoms confirmed the presence of three ester functionalities (δ_C 172.2, 170.8, 170.8), two acetylated quarternary carbons (δ_C 86.5 and 82.4) and a hydroxylated quaternary carbon (δ_C 75.6) forming part of a ring structure. There were seven methine carbons resonating at δ_C 83.8 (acetylated methine group), δ_C 92.0 and 74.9 (ether group) and δ_C 52.3, 42.7, 42.7, 29.0, which formed part of the ring structure. Also forming a part of this apparent ring structure were five methylene groups at δ_C 48.2, 35.5, 32.4, 29.7, 17.4 and five methyl groups at δ_C 23.9, 22.8, 21.5, 22.1, 14.6, were identified. Three acetyl methyls could clearly be seen resonating at δ_C 21.5, 21.1, 20.4. From this data, the molecular formula was calculated as $[(C)_6+(CH)_7+(CH_2)_5+(CH_3)_8+(O)_7+(OH)=482]$ $C_{26}H_{42}O_8$ indicating the presence of six degrees of unsaturation three of which could be accounted for the three acetate groups initially identified. The LRESIMS gave a peak at m/z 505 $[M+Na]^+$ and m/z 423 $[M-CH_3COO]^+$. The accurate mass measurement of m/z 505 was difficult and did not yield the level of accuracy desired, probably due to the rapid loss of CH_3COONa. However, accurate mass measurement at m/z 423 gave 423.2741, Δ=+0.0 calculated for $C_{24}H_{39}O_6$ $[M-CH_3COO]^+$.

With the aid of an HSQC spectrum all protons were assigned to their directly bonded carbon atoms (Table 1). Five substructures were constructed by interpretation of the ^{1}H–^{1}H COSY spectrum (Fig. 1a). The connection between these substructures were established by interpretation of an HMBC spectrum (Fig. 1b and 1c) and all the spin systems were confirmed by data from an HSQC–TOCSY spectrum (Fig. 1d). The HSQC–TOCSY spectrum proved invaluable by providing correlations, which confirmed the ^{1}H–^{1}H COSY substructures and enabled their extension. HMBC correlations from C-10 to H-17, C-12 to H-17, C-15 to H-2, C-4 to H-15, C-8 to H-16 and C-6 to H-16 confirmed the relative positions of the three methyls C-15, C-16 and C-17 on the skeleton. ^{1}H–^{1}H COSY correlations from H-9 to H-10 and HMBC correlations from C-9 to H-10 confirmed the adjacency of C-10 and C-9. Also, HMBC correlations from C-1 to H-2 and C-3 to H-2 together with ^{1}H–^{1}H COSY correlations between H-1 and H-10 confirm the

Table 1. ^{1}H, ^{13}C and 2D NMR data at 400/100 MHz for the 3,11-diacetylated diterpene skeleton in structures **1** and **2a–t** in CD_3OD

	δ^{13}C/ppm, mult	δ^{1}H/ppm, mult, *J* (Hz)	COSY H→H	HMBC C→H	HSQC–TOCSY C→H
1	42.7, d	2.16 dd, 7.2, 12.0	H-12b, H-13a, H-14	H-2, H-10, H-19, H-20	H-1, H-13a
2	92.0, d	3.53 s	—	H-15	H-2
3	86.5, s	—		H-2, H-15	
4a	35.5, t	2.01 ddd, 14.8, 7.7, 1.8	H-4b	H-6, H-15	H-4a/4b, H-5
4b		2.47 m	H-4a		
5	29.7, t	1.45 m	H-6	—	H-5
6	83.8, d	5.56 d, 4.8	H-5	H-16	H-4a, H-6
7	75.6, s	—	—	H-6, H-16	—
8a	48.2, t	1.79 dd, 4.0, 14.8	H-8a/8b, H-9	H-10, H-16	H-8a/8b
8b		1.99 dd, 4.0, 14.8			
9	74.9, d	4.03 ddd, 4.0, 8.0, 11.6	H-8a/8b, H-10	H-2, H-10	H-8a/8b, H-9
10	52.3, t	3.24 t, 7.2	H-9, H-14	H-2, H-17	H-8a/8b, H-10
11	82.4, s	—	—	H-10, H-17	—
12a	32.4, t	1.41 m	H-12a/12b	H-17	—
12b		2.06 m			
13a	17.4, t	1.09 m	—	—	H-12a, H-13a
13b		1.40 m			
14	42.7, d	1.13 m	H-1, H-10	H-2, H-10, H-19, H-20	H-12a, H-13a, H-14
15	22.1, q	1.33 s		H-2	H-15
16	22.8, q	1.20 s	—	—	H-16
17	23.9, q	1.45 s	—	—	H-17
18	29.0, d	1.75 m	H-19, H-20	H-19, H-20	H-12a, H-18, H-19, H-20
19	21.5, q	0.94 d, 6.8	—	H-20	H-19, H-20
20	14.6, q	0.80 d, 6.8	—	H-19	H-19, H-20
21	21.1, q	2.04 s	—	—	—
22	21.5, q	1.95 s	—	—	—
23	170.8, s	—	—	H-21	—
24	170.8, s	—	—	H-22	—

situation of C-1 relative to C-10 and C-2. HMBC correlations from C-11 to H-17, C-7 to H-16, C-4 to H-6 and C-3 to H-15 show the exact positions of the oxygenated carbons C-3, C-6, C-7 and C-11. The lack of any relevant correlations linking the acetate groups to the eunicellin-based skeleton made it difficult to assign their exact positions on the ring. The same problem was reported by Ortega et al.[20] in assigning the structure of palmonine B (**3**) where the three acetates could not be assigned to their exact positions on the ring. In many cases derivatisation has been used to solve this problem, as in the structure determination of klyxumines A and B.[21] Compound **1** cannot be readily derivatised so another solution must be sought. In compound **4** it was easy to assign the position of the acetate group as there was only one possibility.[22] Oxygenated carbons are easily assigned as in sclerophytin A (**5**),[23] but the attachment of acetates can be problematic. Chemical shift evidence suggested that the C-7 position in **1** was not acetylated, as the ^{13}C NMR chemical shift was more shielded relative to the acetylated carbons C-3, C-6 and C-11. Additional evidence for this hypothesis came from a homologue, compound **2a**.

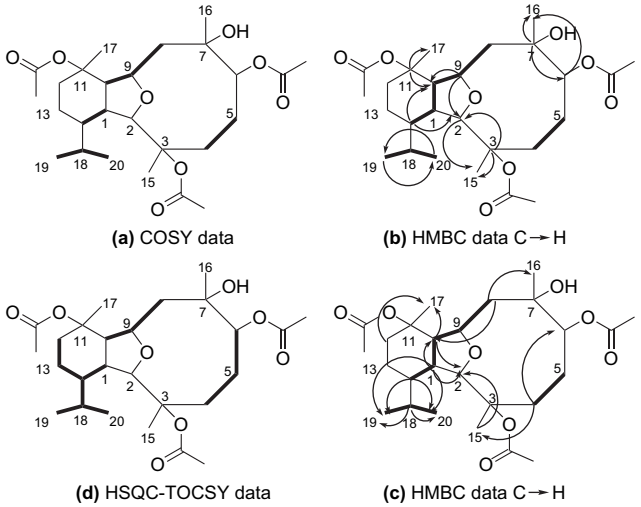

Figure 1. Important 2D NMR correlations for compound **1**.

The ^{1}H NMR of compound **2a** was very similar to that of compound **1**. One of the major differences was the disappearance of one of the acetyl methyls initially observed at δ_H 1.99 (s, 3H) and found from HMBC correlations to be attached to δ_C 172.2 (Table 2). In place of this, a new methylene signal appeared at δ_H 2.26 (t, 2H, J=7.2 Hz). A new methyl signal was also observed at δ_H 0.83 (m, 3H) and two methylene signals were also found at δ_H 1.21 (m, 2H) and 1.24 (m, 2H) (Table 2). The ^{13}C NMR of compound **2a** was made up of 30 ^{13}C signals. The four additional signals compared to compound **1** were found at δ_C 14.1, 22.0, 25.1, 31.8. The main carbon skeleton of **2a** was found to be the same as that of **1**, the new signals arising as a consequence of fatty acid chain incorporation on the acetate group found at δ_C 172.2 in compound **1** and was seen to shift to δ_C 174.2 in compound **2a**. The additional 2D NMR correlations observed for the fatty acid side chain incorporated onto, δ_C 174.2, ester carbonyl group are shown in Figure 2. Most of the 2D NMR data collected for the carbon skeleton of compound **2a** were the same as that shown in Figure 1 for compound **1**. Assigning the exact positions of the acetate groups were a problem in compound **2a** however, the HMBC spectra for a mixture of homologues with the same structure as compound **2a** but with longer fatty acid side chains revealed a correlation from δ_C 174.9 to H-6, which led us to infer that the hexanoyl group was attached at C-6. Another interesting correlation seen in this spectrum was from δ_C 170.8 (attached to the δ_H 2.04, s, 3H) to H-2 suggesting

Table 2. ^{1}H, ^{13}C and 2D NMR data at 400/100 MHz for the acetyl side chains at C-6 in structures **1** in CD_3OD and for **2a** and **2b–f** in $CDCl_3$

	δ^{13}C/ppm, mult	δ^{1}H/ppm, mult, J/Hz	COSY H→H	HMBC C→H	HSQC–TOCSY C→H
Compound ***1***					
1′	172.2, s	—	—	H-2′	—
2′	20.4, q	1.99 s	—	—	H-2′
Compound ***2a***					
1′	174.2, s	—	—	H-2′	—
2′	34.0, t	2.26 t, 7.2	H3′	—	H-2′, H-3′
3′	25.1, t	1.56 m	H2′, ω3-H	H-2′, ω3-H	H-2′, H-3′, ω3-H
ω3	31.8, t	1.21 m	—	ω2-H, ω1-H	—
ω2	22.0, t	1.24 m	H3′	ω1-H	H-2′, ω3-H, ω1-H
ω1	14.1, q	0.83 m	ω3-H	—	ω2-H, ω1-H
Compounds ***2b–f***					
1′	174.9, s	—	—	H-6, H-2′	—
2′	34.8, t	2.17 t, 7.2	H3′	H-3′	H-2′, H-3′, H-4′
3′	25.3, t	1.59 m	H2′	H-2′	H-2′, H-3′, H-4′
$(CH_2)_n$	29.9, t	1.22 s			
ω3	31.9, t	1.24 m	—	ω2-H, ω1-H	ω3-H, ω1-H
ω2	22.9, t	1.27 m	ω4-H	ω1-H	ω4-H, ω2-H, ω1-H
ω1	14.1, q	0.86 m	ω2-H	—	ω4-H, ω3-H, ω2-H, ω1-H

that this acetyl group is substituted on C-3. The remaining acetyl group δ_C 170.8 (attached to the δ_H 1.95, s, 3H) was therefore placed on C-11. From the ^{13}C NMR of compound **2a**, a molecular formula was calculated as $C_{30}H_{50}O_8$ indicating the presence of six degrees of unsaturation. The LRESIMS gave a *m/z* 561, which was measured accurately as 561.3398, Δ=+1.0.

To establish that the relative configuration of **1** was as reported for related compounds **3–5**, the global minimum energy conformation of compound **1** was calculated using a Monte Carlo conformational search (10,000 steps, global minimum shown in Fig. 3).[24] The molecular mechanics calculations indicated H-10 as being cis to H1 (α-position of the ring-downwards). A strong correlation in the T-ROESY spectrum was consistent with this configuration. In the energy-minimised structure H9 was cis to H2 (β-position of the ring-upwards) and no correlations were expected because of the five-membered ring. However, the absence of any T-ROESY correlations between H-9–H-10 and between H-2–H-1 suggested that H-10 and H-1 were in the α-position and H-9 and H-2 in the β-position. The equatorial placement of methyl H-17 in the molecular mechanics calculations was confirmed by the strong correlation in the T-ROESY spectrum between H-17 and the protons H-8′. Strong T-ROESY correlations between isopropyl methyls H-20/H-19 and methyl H-15 confirmed the equatorial positions occupied by these two substituents. Strong correlations were also seen between methyl H-16 and H-8′, which suggested that this methyl substituent was axially placed. The lack of T-ROESY correlations between H-6 and the protons on methyl H-16 corroborated this assumption.

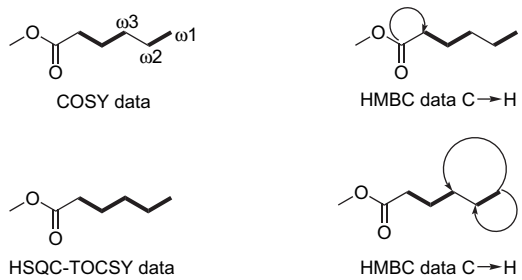

Figure 2. Important 2D NMR correlations for the side chain in compound **2a**.

Analysis of these HPLC fractions by LRESIMS revealed that the parent mixture, which yielded **1** and **2a** was composed of a homologous series of eunicellin-based diterpenoids with the same skeleton as compound **1** but with sequential aliphatic side-chain elongation on one of the ester groups attached to the skeleton (compounds **2a–t**). When the parent mixture was subjected to HPLC effective separation was unachievable, and peaks with the same ^{1}H and ^{13}C NMR were obtained. The mass spectra of these peaks showed them still to be complex mixtures, and therefore the parent mixture was investigated by tandem mass spectrometry (MS/MS). Of the available modes in MS/MS, product ion scanning is the most frequently used. Ions of a particular *m/z* value are selected in the first stage of mass analysis, these precursor ions are fragmented and the product ions resulting from the fragmentation are analysed in a second stage of mass analysis.[25] Less often applied is precursor ion scanning, in which all molecular ions giving rise to the same product ion are identified.

In compounds **2a–t**, two pathways of fragmentation were proposed leading to key product ions at *m/z* 481 (Scheme 1) and *m/z* 423 (Scheme 2). The fragmentation in Scheme 1 was

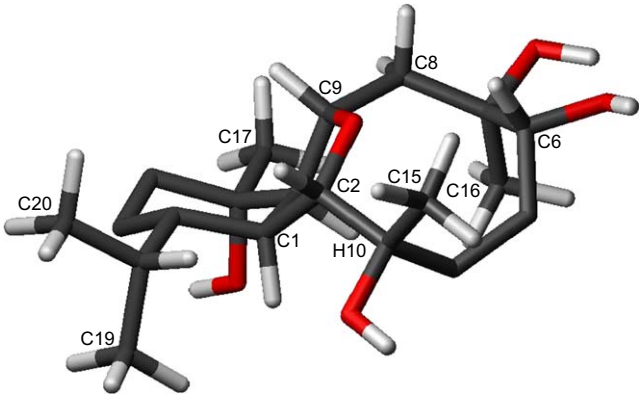

Figure 3. Global energy minimum of compound **1** (for clarity, only key H atoms are shown). Figure was generated using MolMol.[28]

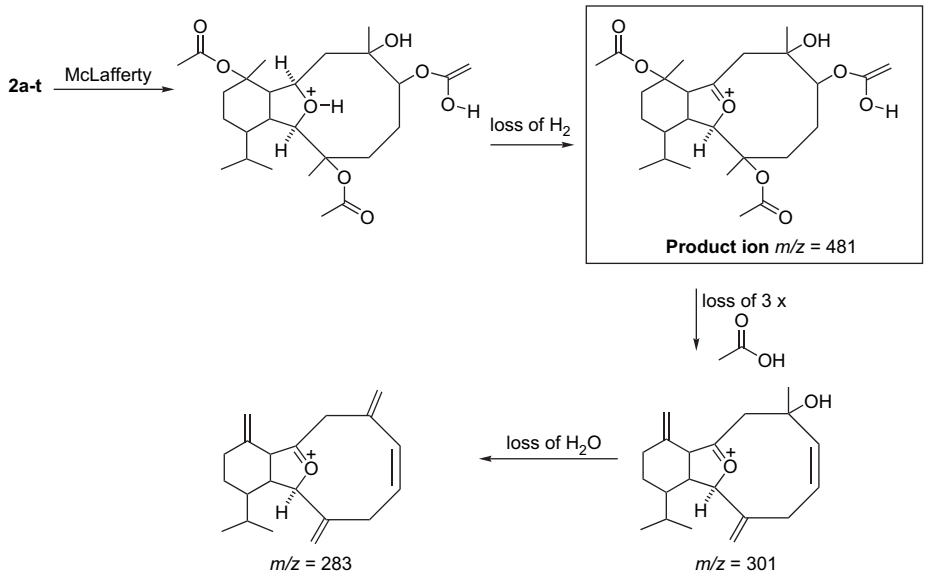

Scheme 1. Positively ionised molecular ions of **2a–t** undergo McLafferty rearrangement with subsequent loss of H_2, which leads to the formation of the onium ion at *m/z* 481. Subsequent fragmentations of *m/z* 481 gives information about its structure.

confirmed by the iterative loss of acetate groups from *m/z* 481 followed by the loss of water as seen in the product ion scan (Fig. 4c). It is evident from Figure 4a, that analysis of the raw MS data would be impossible in this case. The clarification offered by the use of tandem mass spectrometric techniques is invaluable here (Fig. 4b–d). The species at *m/z* 481 (Scheme 1) is the onium ion, which is frequently seen in the spectra of ethers, alcohols and amines. The species at *m/z* 481 loses $3\times CH_3COOH$ to give rise to the species at *m/z* 301, followed by a loss of H_2O giving *m/z* 283. Other fragments of *m/z* 481 can be accounted for as follows: loss of C_2H_2O from the species at *m/z* 421 gives rise to *m/z* 379; loss of C_2H_2O from *m/z* 361 leads to *m/z* 319; loss of H_2O from *m/z* 361 gives the peak at *m/z* 343 and a loss of H_2O from *m/z* 421 gives *m/z* 403.

In Scheme 2 sodiated molecular ions undergo a McLafferty type rearrangement to give a product at *m/z* 505 (Fig. 4b). This species then undergoes a direct cleavage leading to a loss of 82 mass units ($C_2H_3O_2Na$) leaving *m/z* 423. Using the precursor ion scanning strategy on *m/z* 423 we obtained all the precursors, from *m/z* 561 upwards in increments of 14 mass units (Fig. 4b, Table 3). Accurate mass values were obtained for several of these, which agree with the molecular formulae of acetylated compounds **2b–t** with varying lengths of acyl chains (Table 3). In addition it appears that some monounsaturated side chains are also present (e.g., at *m/z* 727 and *m/z* 741). In a similar fashion, we obtained the precursors of *m/z* 481 (Fig. 4d), but the data is less clear than the *m/z* 423 precursor ion scan and not easily interpreted (Fig. 4b).

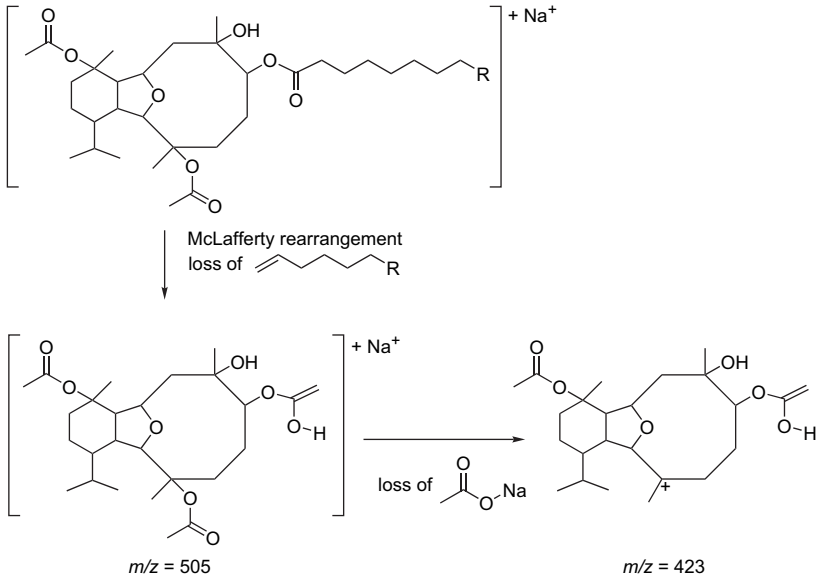

Scheme 2. Sodiated molecular ions of **2a–t** undergo McLafferty rearrangement with the concomitant loss of the appropriate neutral molecule and formation of the species at *m/z* 505, which subsequently loses a mass of 82 giving rise to the species at *m/z* 423.

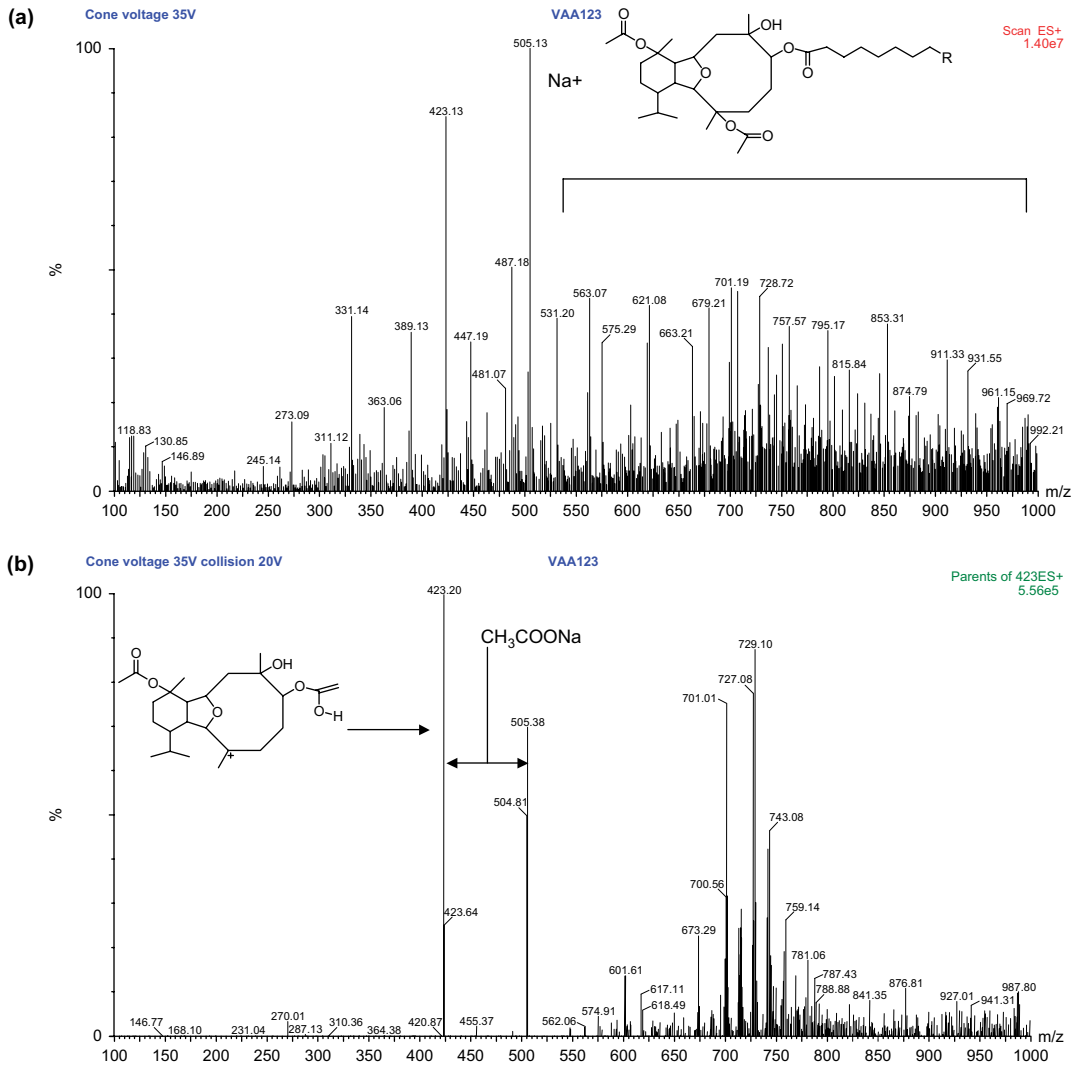

Figure 4. MS and MS/MS spectra of parent fraction of acetylated eunicellin diterpenes **2a–t**: (a) MS spectrum; (b) precursor ion scan of *m/z* 423; (c) product ion scan of *m/z* 481; and (d) precursor ion scan of *m/z* 481.

To confirm our conclusions obtained from the tandem mass spectra, we obtained full 1D and 2D NMR data on the parent mixture analysed by tandem mass spectrometry. The diterpene skeleton was found to be identical to **1** and additional data was obtained for the fatty acid side chains (Table 2). The data for the termini of the fatty acid chain were clear, but the central methylenes of the chain were contained within the CH_2 envelope at δ_H 1.22 and δ_C 29.9. An HMBC correlation from C-1′ to H-6 places the acyl chain at C-6. Table 3 indicates the mass data for the homologous series of long chain eunicellin diterpenes **2a–t**.

2.1. Biological activity data

Compared to their eleutherobin and sarcodictyin counterparts, eunicellin-based diterpenoids exhibit moderate cytotoxicities. Sclerophytin A (**5**) exhibits the most remarkable cytotoxicity profile, active against L1210 leukaemia cell-lines at a concentration of 1 ng/mL.[23] Other examples include **4** reported by Shin et al.[22] to exhibit moderate in vitro cytotoxicity against human tumour cell-lines. The ED_{50} values of this compound were 12.7, 21.3, 11.6 and 13.9 μg/mL against A-549 non-small cell lung cancer, SKOV-3 ovarian cancer, SK-MEL-2 melanoma and HCT-15 colon cancer cell-lines, respectively. The highly acetylated eunicellin-based diterpenoids do not exhibit interesting cytotoxicity profiles with the exception of palmonine B, which was originally reported by Ortega et al.[20] to have activity against P-388 and MEL28 cells with (ED_{50}=5 μg/mL). Compounds **1** and **2a** were evaluated in vitro at the Ford Cancer Center, for their differential cytotoxicity in the soft agar assay.[26,27] They were found to be inactive against the murine colon adenocarcinoma-38 (C-38) cells. The compounds exhibited no murine solid tumour selectivity relative to murine normal cells.

3. Conclusion

The series of compounds identified adds to the growing number of diterpenes of this type isolated from the class Alcyonaria. The difference in the oxygenation pattern is of interest, but it is notable that an entire homologous series appears to be generated biosynthetically, perhaps with a function to allow lipid transport or membrane anchoring of these compounds. These compounds could not have been adequately identified without tandem mass spectrometry techniques,

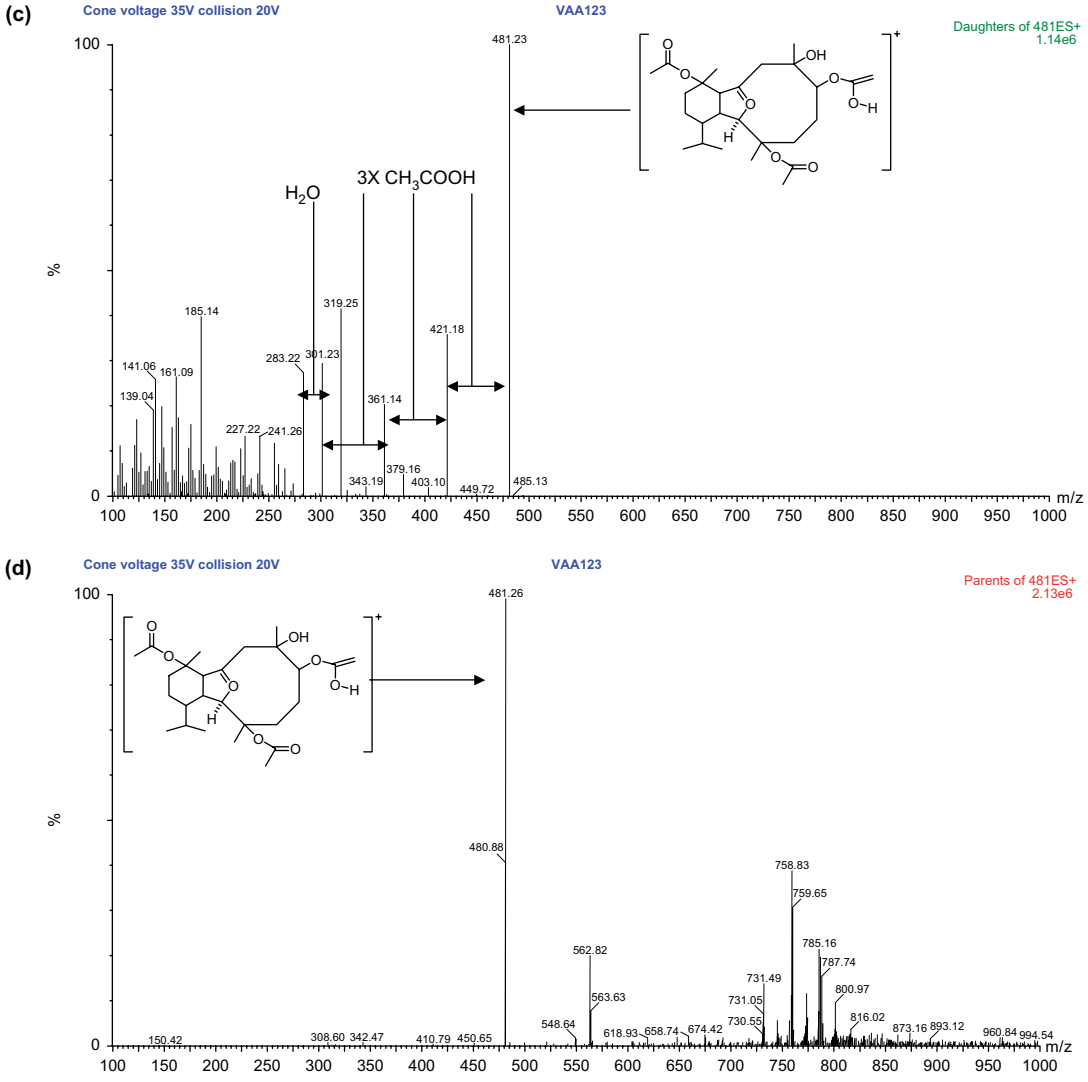

Figure 4. (*continued*)

Table 3. Masses observed for acetyl side chains at C-6 in compounds **2a–t**

Compounds	*n*	$[RCOO]^-$	$[RCOO]^-$ nominal mass	Molecular formula for $[M+H]^+$ or $[M+Na]^+$	Calculated nominal mass	Observed mass (LRESIMS/HRESIMS)	Accurate mass error (ppm)
2a	4	$C_6H_{11}O_2$	115	$C_{30}H_{50}O_8Na$	561	561.3398	+1.0
2b	5	$C_7H_{13}O_2$	129	$C_{31}H_{52}O_8Na$	575	575	
2c	6	$C_8H_{15}O_2$	143	$C_{32}H_{54}O_8Na$	589	589	
2d	7	$C_9H_{17}O_2$	157	$C_{33}H_{56}O_8Na$	603	603	
2e	8	$C_{10}H_{19}O_2$	171	$C_{34}H_{58}O_8Na$	617	617	
2f	9	$C_{11}H_{21}O_2$	185	$C_{35}H_{60}O_8Na$	631	631	
2g	10	$C_{12}H_{23}O_2$	199	$C_{36}H_{62}O_8Na$	645	645	
2h	11	$C_{13}H_{25}O_2$	213	$C_{37}H_{64}O_8Na$	659	659	
2i	12	$C_{14}H_{27}O_2$	227	$C_{38}H_{66}O_8Na$	673	673.4658	+1.2
2j	13	$C_{15}H_{29}O_2$	241	$C_{39}H_{68}O_8Na$	687	687	
2k	14	$C_{16}H_{31}O_2$	255	$C_{40}H_{70}O_8Na$	701	701.4970	+0.9
2l	15	$C_{17}H_{33}O_2$	269	$C_{41}H_{72}O_8Na$	715	715.5102	−2.4
2m	16	$C_{18}H_{35}O_2$	283	$C_{42}H_{74}O_8Na$	729	729.5279	+0.5
2n	17	$C_{19}H_{37}O_2$	297	$C_{43}H_{76}O_8Na$	743	743.5432	+0.8
2o	18	$C_{20}H_{39}O_2$	311	$C_{44}H_{78}O_8Na$	757	757	
2p	19	$C_{21}H_{41}O_2$	325	$C_{45}H_{80}O_8Na$	771	771	
2q	20	$C_{22}H_{43}O_2$	339	$C_{46}H_{82}O_8Na$	785	785	
2r	21	$C_{23}H_{45}O_2$	353	$C_{47}H_{84}O_8Na$	799	799	
2s	22	$C_{24}H_{47}O_2$	367	$C_{48}H_{86}O_8Na$	813	813	
2t	23	$C_{25}H_{49}O_2$	381	$C_{49}H_{88}O_8Na$	827	827	

which are powerful tools for the analysis of a homologous series of compounds. On occasion it proves difficult to achieve effective separation of metabolites by chromatographic methods, and in these instances we must rely on the separating power afforded by tandem mass spectrometric techniques. In this study we have shown the power of the precursor ion scan, in which all parent molecules giving rise to the same product ion are identified. The simplification this technique provides compared to analysing raw spectra is unparalleled. As was shown, the NMR data for this intractable mixture did not provide sufficient data to allow a full analysis of the structures of the homologous series, whereas this was facile using tandem mass spectrometric techniques.

4. Experimental

4.1. General experimental procedures

IR spectra were measured on an Ati Mattson Genesis Series FTIR machine. ^{1}H, ^{13}C and all 2D NMR experiments were recorded on a Varian Unity INOVA 400 MHz spectrometer, in CD_3OD or $CDCl_3$. Mass spectrometry/Mass spectrometry spectra were obtained from a Waters Micromass Quattro Premier XE instrument equipped with a MassLynx 4.0 software. LRESIMS were obtained from a Waters ZQ-4000 low-resolution single quadruple mass spectrometer with API capability; mass range *m/z* 4000; unit resolution. (*Waters-Micromass, Manchester, UK*). All accurate mass measurements were obtained from a Finnigan MAT 900 XLT high resolution double focussing mass spectrometer with tandem Ion Trap and EI, CI, LSIMS, API capability (*Thermo-Finnigan, Bremen, Germany*). HPLC separations were carried out using a Thomsons Scientific Silica-EL5-30784 Silica EXSIL 5 μm×25 cm×10 mm i.d. column and Spectraseries P100 isocratic pump and monitored using a Waters Associates, Inc. (Milford Mass) Differential Refractometer R401.

4.2. Biological material

The sample of *Acalycigorgia* sp. was collected by the Australian Institute of Marine Science in Thailand at 07 41.2 N; 98 46.4 E on 1 June 1990 at 15 m. Taxonomic identification was carried out by Phil Aderslade at the Museum of the Northern Territories and vouchers (COO6609) are kept at both the National History Museum in Washington DC, USA and at the Queensland Museum in Brisbane, Australia. Collected specimens were stored at −20 °C until used.

4.3. Extraction and isolation

The frozen sample was ground into a coarse powder and extracted with H_2O. The ground-up tissue was lyophilised and extracted using a 1:1 mixture of CH_2Cl_2/MeOH. The solvent was removed under reduced pressure leaving 1.47 g of organic extract, which was subjected to a solvent partition. The extract (1.47 g) was partitioned between water and CH_2Cl_2. The solvent was removed from the CH_2Cl_2 layer and the resulting oil was partitioned between *n*-hexane and 10% aqueous MeOH. The 10% aqueous MeOH layer was extracted three times with equal volumes of *n*-hexane. The solvent was removed from the *n*-hexane layer and the resultant extract (0.83 g) was subjected to normal phase flash chromatography with gradient elution. Gradient elution was achieved by first flushing the silica gel column with 100% hexane and collecting all the metabolites that eluted, this was then followed by a 50/50 v/v mixture of hexane/ethylacetate then a 100% solution of ethylacetate before finally flushing all the remaining material off the column with 100% methanol. The gradient elution protocol was designed in order to elute the least polar metabolites first. The resultant fractions listed in order of increasing polarity were FHFS1-1/7 (least polar metabolites=230 mg), FHFS2-8/20 (300 mg), FHFS3-21/48 (200 mg) and FHFS4-49/71 (most polar metabolites=100 mg). Many compounds were isolated from all four fractions but the compounds described herein were obtained from the FHFS1-1/7, which was subsequently subjected to size exclusion chromatography by Sephadex LH-20 gel using a 1:1 mixture of MeOH:CH_2Cl_2. Resulting fractions of interest were further purified by repeated normal phase HPLC using 85/15 and 90/10 v/v mixtures of hexane and ethylacetate as eluents. A total of 6.75 mg of compound **1** and 9.85 mg of compound **2a** was fortuitously collected after several HPLC runs.

4.4. Biological assay

Murine colon adenocarcinoma-38 (C-38) cells and the corresponding murine normal cells CFU (M) were inoculated on different Petri dishes. Circular-shaped filter disks (impregnated with test material at dosages from 50 to 100 μg/disk) were placed at the ends of different Petri dishes inoculated with the two cell types under investigation. The test materials (compounds **1** and **2a**) were solubilised in 100% DMSO before they were impregnated into the filter disks and allowed to dry overnight before use. The plates were incubated for 7–10 days and examined by an inverted stereomicroscope (10×) for the measurement of 'zones of inhibition'. Zones of inhibition were defined by measuring the distance in millimetre from the edge of the filter disk to the beginning of normal-sized colony formation. The assay is designed to determine large differences in the relative sensitivity of leukemias, solid tumours and normal cell for a given sample by comparison of the magnitude of inhibition zones. Generally, high values of inhibition zones are desirable. However, high values of inhibition zones for solid tumour cells were preferred over those for leukaemia cells (solid tumour selective). The diameter of the filter disk, 6.5 mm, is arbitrarily taken as 200 units therefore, 1 mm ≡ 30.8 units. A zone of less than 100 units taken as the extract was of insufficient activity to be of further interest. A difference in zones between solid tumour cells and either normal or leukaemia cells of 250 units defined solid tumour selective compounds.

4.4.1. Compound 1. Colourless oily substance, 6.75 mg; IR ν_{max} 3435 (b), 2930, 1728; NMR data (Table 1); LRESIMS *m/z* 505 $[M+Na]^+$; HRESIMS *m/z* 423.2741 $[M-CH_3COONa]^+$, Δ=+0.0 calculated for $[C_{24}H_{39}O_6]^+$.

4.4.2. Compound 2a. Oily substance, pale yellow when in solution, 9.85 mg; IR ν_{max} 3432 (b), 2925, 1728; NMR data (Table 1); LRESIMS *m/z* 561 $[M+Na]^+$; HRESIMS *m/z* 561.3398 $[M+Na]^+$, Δ=+1.0 calculated for $C_{30}H_{50}O_8Na$.

Acknowledgements

This work was supported by the NCI Open Repository Programme and the Australian Institute of Marine Science by providing the organic extract of *Acalycigorgia* sp. The EPSRC National Mass Spectrometry Centre, University of Wales Swansea, provided LRESIMS and all accurate mass measurements. Prof. Fred Valeriote of the Ford Cancer Center, Detroit, USA is thanked for biological assay data.

References and notes

1. Kennard, O.; Watson, D. G.; Riva di Sanseverino, L.; Tursch, B.; Bosmans, R.; Djerassi, C. *Tetrahedron Lett.* **1968**, *9*, 2879–2884.
2. Mancini, I.; Guella, G.; Zibrowius, G.; Pietra, F. *Helv. Chim. Acta* **2000**, *83*, 1561–1575.
3. Rao, D. S.; Sreedhara, C.; Rao, D. V.; Rao, C. B. *Indian J. Chem., Sect. B* **1994**, *33*, 198–199.
4. Rodriguez, A. D.; Cóbar, O. M. *Tetrahedron* **1995**, *51*, 6869–6880.
5. D'Ambrosio, M.; Guerriero, A.; Pietra, F. *Helv. Chim. Acta* **1988**, *71*, 964–976.
6. Ketzinel, S.; Rudi, A.; Schleyer, M.; Benayahu, Y.; Kashman, Y. *J. Nat. Prod.* **1996**, *59*, 873–875.
7. Groweiss, A.; Look, S. A.; Fenical, W. *J. Org. Chem.* **1988**, *53*, 2401–2406.
8. Sharma, P.; Alam, M. *J. Chem. Soc., Perkin Trans. 1* **1988**, 2537–2540.
9. Lin, Y. C.; Bewly, C. A.; Faulkner, D. J. *Tetrahedron.* **1993**, *49*, 7977–7984.
10. Miyamoto, T.; Yamada, K.; Ikeda, N.; Komori, T.; Higuchi, R. *J. Nat. Prod.* **1994**, *57*, 1212–1219.
11. Ochi, M.; Yamada, K.; Kataoki, K.; Kotsuki, H.; Shibata, K. *Chem. Lett.* **1992**, 155–158.
12. Fusetani, N.; Nagata, H.; Hirota, H.; Tsuyuki, T. *Tetrahedron Lett.* **1989**, *30*, 7079–7082.
13. Ochi, M.; Futatsugi, K.; Hotsuki, H.; Ishi, M.; Shibata, K. *Chem. Lett.* **1987**, 2207–2210.
14. Patrick, B.; Paquette, L. A. *Heterocycles* **1998**, *49*, 531–556.
15. He, L.; George, A.; Horwitz, O. B.; Horwitz, B. S. *Drug Discovery Today* **2001**, *6*, 1153–1164.
16. Friedel, M.; Goltz, G.; Mayer, P.; Lindel, T. *Tetrahedron Lett.* **2005**, *46*, 1623–1626.
17. Nicolau, K. C.; Hepworth, D.; King, N. P.; Finlay, M. R. V. *Pure Appl. Chem.* **1999**, *71*, 989–997.
18. Blunt, J. W.; Copp, B. R.; Munro, M. H. G.; Northcote, P. T.; Prinsep, M. R. *Nat. Prod. Rep.* **2006**, *23*, 26–78.
19. Blunt, J. W.; Munro, M. H. G. MarinLit, vpc2.6, Canterbury, New Zealand, 2001.
20. Ortega, M. J.; Zubia, E.; Salva, J. *J. Nat. Prod.* **1994**, *57*, 1584–1586.
21. Chill, L.; Berrer, N.; Benayahu, Y.; Kashman, Y. *J. Nat. Prod.* **2005**, *68*, 19–25.
22. Seo, Y.; Rho, J.-R.; Cho, K. W.; Shin, J. *J. Nat. Prod.* **1997**, *60*, 171–174.
23. Sharma, P.; Alam, M. *J. Chem. Soc., Perkin Trans. 1* **1988**, 2537–2540.
24. Mohamadi, F.; Richards, N. G. J.; Guida, W. C.; Liskamp, R.; Lipton, M.; Caulfield, C.; Chang, G.; Hendrickson, T.; Still, W. C. *J. Comput. Chem.* **1990**, *11*, 440–467.
25. Crews, P.; Rodriguez, J.; Jaspars, M. *Organic Structure Analysis*; Oxford University Press: New York, NY, 1998; p xxiv+552.
26. Valeriote, F.; Corbett, T.; LoRusso, P.; Moore, R. E.; Scheuer, P.; Patterson, G.; Paul, V.; Grindey, G.; Bonjouklian, R.; Pearce, H.; Stuffness, M. *Int. J. Pharmacol.* **1995**, *33*, S59.
27. Valeriote, F.; Corbet, T.; Edelstein, M.; Baker, L. *Cancer Invest.* **1996**, *14*, 124–125.
28. Koradi, R. M. B.; Wuthrich, K. *J. Mol. Graph.* **1994**, *14*, 51–59.